Advanced Physics Lab I

Lab Report #4

Group 1
Noah Horne, Luka Burduli

7.10.2024

Dr. Veit Wagner
Tim Jesko Söcker

We hereby declare that we (Luka Burduli and Noah Horne) are the sole authors of this lab report and have not used any sources other than those listed in the bibliography and identified as references throughout the report.

_____ _____

Contents

1 Abstract

This experiment aimed to calculate the thermal and electrical conductivities (λ, σ) of Copper, Aluminum and Steel, while concomitantly verifying the Wiedemann-Franz law through the calculation of the Lorenz Number L. The thermal conductivities of Copper, Aluminum and Steel were found to be $(340.9 \pm 13.16)[Wm^{-1}K^{-1}], (161.5 \pm 6.8)[Wm^{-1}K^{-1}]$ and $(46.4 \pm 5.15)[Wm^{-1}K^{-1}]$ respectively. Likewise, the electrical conductivities σ of these metals were calculated to be $(8.40 \pm 0.69) \cdot 10^6[Sm^{-1}]$, $(6.54 \pm 0.51) \cdot 10^7[Sm^{-1}]$ and $(4.29 \pm 0.338) \cdot 10^7[Sm^{-1}]$. From these values, the associate Lorenz number approximations derived from the Wiedemann-Franz law were: $(1.86 \pm 0.368) \cdot 10^{-8}[W\Omega K^{-2}]$,$(1.76 \pm 0.22) \cdot 10^{-8}[W\Omega K^{-2}]$,$(1.24 \pm 0.15) \cdot 10^{-8}[W\Omega K^{-2}]$. Along the way, associated constants such as the specific heat capacity of the calorimeter used and rate of change of calefaction were taken into account. Overall, the measurements found were slightly systematically offset, but still reflected the real world properties of the three metals.

2 Introduction & Theory

This investigation primarily focuses on the thermal and electrical conductivity λ, σ of Copper, Aluminum and Steel rods. By calorimetrically gathering time-dependent measurements of the heat flow in a rod removed from its steady state–using two calorimeters on either end of the rod–the thermal conductivity is calculated. To calculate the electrical conductivity, the resistivity of the rods are determined, and the electrical conductivity is immediately derived from the developed theory. The electrical conductivity σ is defined by measurements of the resistance R of the rods and its length l and cross-sectional area A. It is defined as a materials ability to conduct electricity efficiently. It can also be described as the reciprocal of the resistivity ρ, and is given by:

$$\sigma = \frac{1}{\rho} = \frac{l}{A \cdot R} \tag{1}$$

By contrast, heat in metals is conducted two main entities: electrons and phonons. Phonons are small vibrations in crystal lattice of the metal causing the transfer of energy. Electrons on the other hand, transfer heat through their movement in the metal. At room temperature, the mean free path of electrons is much greater than that of the phonons (which are fixed in the lattice), which implies that the electrons serve as the primary conductors of heat in metals. As one may have already assumed, due to the crucial role that electrons play in the conduction of heat, the electrical conductivity and thermal conductivity are associated quanitites. As the mean free path of phonons and electrons is additionally dependent on temperature, it is clear that the relationship between therman and electric conductivity also acknowledges temperature. With

these relationships, the Wiedemann-Franz law is established:

$$\frac{\lambda}{\sigma} = L \cdot T_0 \tag{2}$$

Here, L is the Lorenz number ($L = \frac{\pi^2}{3} \cdot \frac{k_B^2}{e^2} \approx 2.4 \cdot 10^{-8} \frac{W\Omega}{K^2}$) and k_B is the Boltzmann constant, and e is the elementary charge. It is crucial to note that this relationship is only valid for specific temperature that are above the so-called Debye temperature. Should the temperature the conductivities are measured at ever be below the Debye temperature, the ratio of conductivities becomes less than $L \cdot T_0$ (Wagner & Söcker, 2024).

The thermal conductivity λ of a medium is defined by its' ability to conduct heat Q over time. The process of heat conduction, or conducting heat, can be described as the flow of heat energy due to a causal imbalance of temperature (Wagner & Söcker, 2024). To formally describe the flow of heat energy, the heat flux $\vec{q}$ is introduced, a proportional quantity to the difference in absolute temperature. As aforementioned, the thermal conductivity λ serves as a measure for the ability to conduct heat, and so expressing this relationship, the following equation is formulated.

$$\vec{q} = -\lambda \vec{\nabla} T \tag{3}$$

Additionally, the heat energy Q conducted by the heat flux per unit time $\frac{dQ}{dt}$ can be described as the surface integral of the heat flux $\vec{q}$ (Wagner & Söcker, 2024). One integrates over the thermo-conductive surface to achieve the result below.

$$\frac{dQ}{dt} = \oint_S \vec{q} \cdot d\vec{S} \tag{4}$$

By substituting equation 3 into equation 4, one achieves another useful expression of the change in heat energy $\frac{dQ}{dt}$ over time.

$$\frac{dQ}{dt} = -\lambda A \frac{dT}{dx} \tag{5}$$

Here, $\frac{dT}{dx}$ is the change in temperature (temperature gradient) along the rod, x is the length-wise position on the rod, A is defined as the cross-sectional area of the rod, and λ is the heat conductivity. By calculating the change in heat energy $\frac{dQ}{dt}$ and the temperature gradient $\frac{dT}{dx}$ (along with A) one can directly compute the heat conductivity of the metal. While this definition is close to sufficient, it is possible to make it more applicable to the experimental method of this investigation. For one, the procedure of the experiment involves the use of calorimeters with an unknown specific heat capacity C. To find the specific heat capacity of the calorimeter C, the conservation of heat energy Q is used in a mixing experiment involving two masses of water with differing temperature. The change in energy ΔQ of a mass m with specific heat capacity c

for a change in temperature ΔT is given by:

$$\Delta Q = mc\Delta T \tag{6}$$

One can then apply equation 6 directly to the mixing setup. Define c_w as the specific heat capacity of water and C as the specific heat capacity of the calorimeter where the water is held, which is unknown. Furthermore, let $m_{w,cold}$,$m_{w,hot}$ denote the masses of the cold and hot water respectively, and $T_{hot}, T_{cold}, T_{mix}, T_{cal}$ denote the temperatures of the hot, cold, and mixed water and the temperature of the calorimeter respectively. Then, by the conservation of heat energy for each mass of water and the calorimeter:

$$c_w \cdot m_{w,hot} \cdot (T_{hot} - T_{mix}) = C \cdot (T_{mix} - T_{cal}) + c_w \cdot m_{w,cold} \cdot (T_{mix} - T_{cold}) \tag{7}$$

Rearranging equation 7 and solving for the specific heat capacity of the calorimeter one achieves:

$$C = \frac{c_w \cdot m_{w,hot} \cdot (T_{hot} - T_{mix}) - c_w \cdot m_{w,cold} \cdot (T_{mix} - T_{cold})}{T_{mix} - T_{cal}} \tag{8}$$

To make the model of the metal rod even more precise, we can also strengthen the definition of the heat gradient $\frac{dT}{dx}$ in formula 5. When considering a straight, cylindrical metal rod of length l and cross-sectional area A, the steady-state ($\frac{dT}{dt} = \text{const.}$) of the metal rod occurs when the temperature distribution $T(x)$ between the two ends (boundary conditions T_1, T_2) is linear with respect to the intermediate position x between either end of the rod. This steady state occurs when a source of heat energy and a sink of heat energy are placed on either side of the rod, allowing heat to flow lengthwise. The steady-state temperature distribution of a metal rod can be formulaically described as:

$$T(x) = \frac{T_2 - T_1}{l} \cdot x + T_1 \tag{9}$$

Note that the equation above implicitly then defines a 'steady-state' rate of change of temperature with respect to position along the rod $\frac{dT}{dx}$, given clearly by:

$$\frac{dT}{dx} = \frac{T_2 - T_1}{l} \tag{10}$$

With the steady state heat gradient along the metal rod now well defined, one must also account for the effects of the external environment, more specifically, the calefaction of the rod due to the surrounding air. In the context of the investigation, calefaction refers to the loss of heat energy due to the surrounding air of the system. As the air has its own temperature and can be heated, it is possible for the air to introduce or remove energy from the system. During the investigation, an experiment is conducted to determine the rate of calefaction $\frac{dQ_R}{dt}$ by analyzing the temperature T_{cf} of ice cold water in a calorimeter exposed to the air of the laboratory. From

the manual, it is stated that the heat energy dQ_R absorbed by the water and calorimeter sourced from the environment is given as:

$$dQ_R = (c_w \cdot m_{w,cf} + C) \cdot dT_{cf} \tag{11}$$

In equation 11, $m_{w,cf}$ is defined as the mass of the water in the calorimeter during the calefaction experiment (Wagner & Söcker, 2024). Decorating both sides of equation 11 with the time differential dt, one achieves a differential equation that describes the calefaction rate $\frac{dQ_r}{dt}$ in terms of the rate of temperature loss $\frac{dT_{cf}}{dt}$.

$$\frac{dQ_R}{dt} = (c_w \cdot m_{w,cf} + C) \cdot \frac{dT_{cf}}{dt} \tag{12}$$

As one can measure the temperature of water with respect to time by taking a series of measurements with correlation to time, the slope of the linear relationship between the rate of calefaction $\frac{dQ_R}{dt}$ and change in temperature $\frac{dT_{cf}}{dt}$ can be found to be $(c_w \cdot m_{w,cf} + C)$. As the constants for the heat capacity of water and calorimeter c_w and C are known, and the mass of the water used $m_{w,cf}$ is known, the rate of calefaction $\frac{dQ_R}{dt}$ can be easily calculated after the mixing experiment.

Lastly, one can combine the notions of the calefaction and the heat energy loss into a single equation for the context of the experiment. As derived from the *Advanced Physics Lab I* manual, the equation for the loss of heat energy at constant room temperature T_r is given as:

$$\frac{dQ}{dt} = \underbrace{\left.\frac{dQ}{dt}\right|_{T_0}}_{\text{Due to hot water}} - \underbrace{\left.\frac{dQ_R}{dt}\right|_{T_0}}_{\text{Calefaction}} = \underbrace{(c_w \cdot m_w + C) \cdot \left.\frac{dT_{tot}}{dt}\right|_{T_0}}_{\text{Due to hot water}} - \underbrace{(c_w \cdot m_{w,cf} + C) \cdot \left.\frac{dT_{cf}}{dt}\right|_{T_0}}_{\text{Calefaction}} \quad \text{for } T_r = \text{ const.} \tag{13}$$

With this equation one can completely describe the loss of heat energy through known empirical measurements. To calculate the heat conductivity λ, one can equate the right hand side of equation 13 with the definition of $\frac{dQ}{dt}$ in formula 5, substituting the definition of $\frac{dT}{dx}$ from equation 10. Below is the equality.

$$-\lambda A \frac{dT}{dx} = (c_w \cdot m_w + C) \cdot \left.\frac{dT_{tot}}{dt}\right|_{T_0} - (c_w \cdot m_{w,cf} + C) \cdot \left.\frac{dT_{cf}}{dt}\right|_{T_0} \tag{14}$$

When one solves for the thermal conductivity λ, it is given as:

$$\lambda = \frac{(c_w \cdot m_w + C)\frac{dT_{tot}}{dt}|_{T_0} - (c_w \cdot m_{w,cf} + C) \cdot \frac{dT_{cf}}{dt}|_{T_0}}{-A \cdot \frac{T_2 - T_1}{l}} \tag{15}$$

Note that all values in formula 15 can be empirically determined and/or are known, and therefore can be found through sufficient investigation.

3 Experimental Procedure

This experiment aims to calculate the thermal and electrical conductivity of three metal rods: Copper, Steel, and Aluminum. To calculated the thermal conductivity of each rod, formula 15 is applied. However, to apply the formula specific values must be calculated and applied. In equation 15, the value of the specific heat capacity of the calorimeter C must be known, the rate of change of temperature due to calefaction $\frac{dT_{cf}}{dt}$, the rate of change of the temperature of the rod $\frac{dT_{tot}}{dt}$, and the masses of water for each respective experiment.

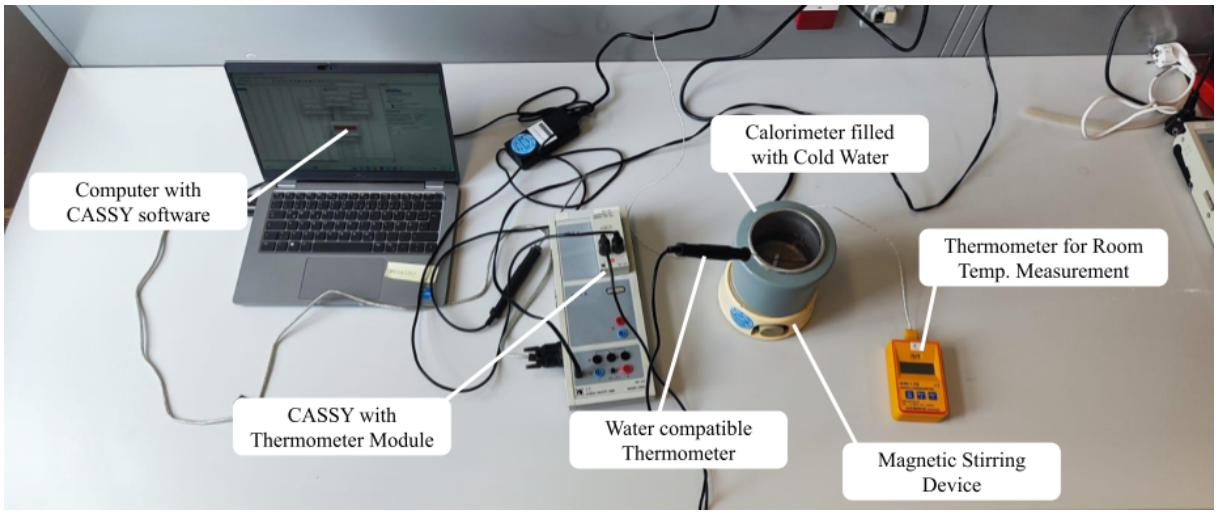

Figure 1: Setup for the Determination of the Rate of Calefaction $\frac{dQ_R}{dt}$

The first of these constants to be determined is the rate of change of temperature due to calefaction $\frac{dT_R}{dt}$, furthermore the rate of calefaction $\frac{dQ_R}{dt}$. Before taking measurements, the mass of the calorimeter was determined through the use of a digital scale. As seen in figure 1, ice cold water (at $0C^\circ$) was placed into a calorimeter equipped with a magnetic stirrer and temperature probe. The temperature probe was connected to a CASSY which monitored the temperature over time. The cold water was then left to sit for approximately 15 minutes with exposure to the surrounding air, taking measurements every 30 seconds. After this process was complete, the combined mass of the water and calorimeter was measured to determine the mass of the water $m_{w,cf}$ via subtraction. The slope of the resulting plot $\frac{\Delta T_{cf}}{\Delta t}$ exactly represents the rate of change of temperature due to calefaction $\frac{dT_{cf}}{dt}$. After the rate of temperature change was found, the rate of calefaction $\frac{dQ_r}{dt}$ was respectively determined through the application of formula 12 after having calculated the specific heat capacity of the calorimeter.

During the 15 minute measuring process of the rate of calefaction, the automatic control of the heater was developed. Through the use of a relay module attached to the CASSY voltage output, the flow of AC current for an AC power strip was controlled. By specifying a parameter for the voltage output of the CASSY, the heater was programmed to only power itself

when specific temperature conditions are met. It was noticed during this investigation that the temperature of the water would continue to rise even after the heater was turned off. This rise was likely due to the stored energy in the metal which continued to transfer to the water of the calorimeter. By exploiting this overshooting phenomena–which was measured to overshoot by approximately 2 to 3 degrees–a parameter was set to automatically turn on the heater when the temperature probe measured below 90 degrees. Setting the temperature of the hot calorimeter to a range between 90 and 93 degrees C° allowed for the sustained heating of the contained water without the consequences of severe evaporation. This automatic control would be used later for providing a consistent boundary condition for the metal rod in its' quasi-steady state.

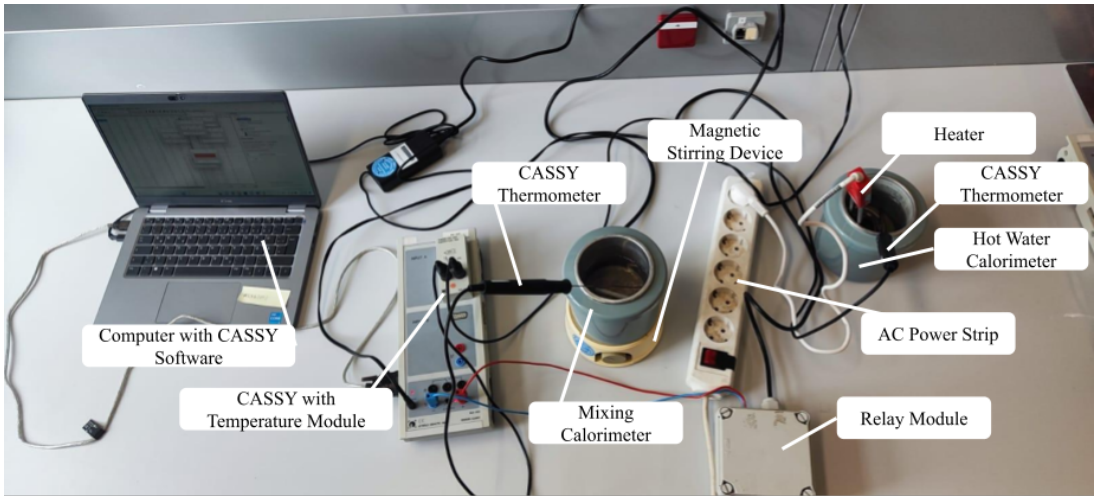

Figure 2: Mixing Setup to Determine the Specific Heat Capacity C of the Calorimeter

To determine the specific heat capacity C of the calorimeter, the property of conservation of thermal energy Q was used in a mixing experiment. As observed in figure 2, two calorimeters held the hot and cold water masses m_{hot}, m_{cold} respectively. Each calorimeter was equipped with its own temperature probe to measure the change its change in temperature. First, the mixing calorimeter was filled with cold water of temperature T_{cold}, and m_{cold} was found by measuring the mass of the filled calorimeter. After heating up the water to a sufficiently hot temperature T_{hot}, the CASSY temperature measurement was started, and measurements were taken every second. Immediately, the hot water was poured into the calorimeter containing the cold water, and the resultant temperature of the mixture T_{mix} was measured by taking the average of the CASSY's time measurements after mixing. The combined mass of the mixture was measured as well to determine the mass of the hot water m_{hot} by subtracting the mass of the calorimeter with cold water from the total mixed mass. With all measurements acquired, the values were substituted into formula 8. This experiment was then performed 5 times, and the best 3 were chosen to be taken in an unweighted average for the final value of the specific heat capacity of the calorimeter C.

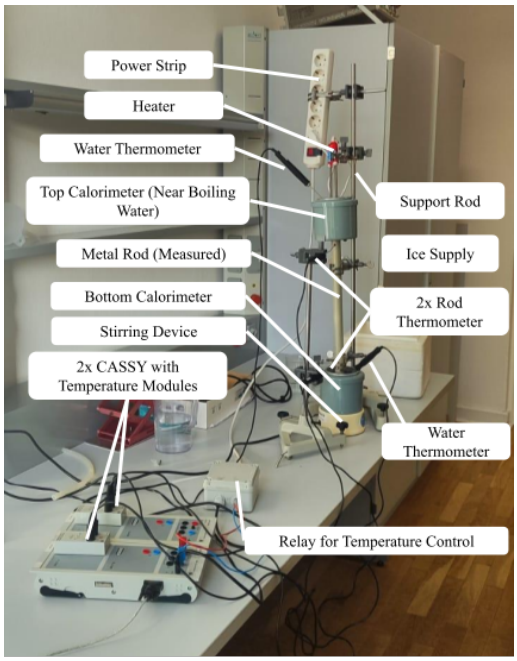

Figure 3: Setup for the Determination of the Rate of Change of Temperature for Quasi-steady State

The last aspect of the thermal conductivity investigation measured the unknown value of the total rate of change of the metal rod in its quasi-steady state, $\frac{dT_{tot}}{dt}$. To do so, the rod was first placed into its steady state by fixing its top and bottom ends to two calorimeters, as seen in figure 3. Four distinct temperature probes were used to measure the temperature of the top calorimeter, bottom calorimeter, top rod, and bottom rod. The temperature probes fixed to the rod are shown in figure 3, and are used to calculate the thermal gradient $\frac{dT}{dx}$ of the rod. To better the thermal conduction between the calorimeters and the rod, thermal conduction paste was placed in between the contact points. Using the pre-established automatic control of the top calorimeter, the temperature of the top of the rod was fixed between $90C^{\circ}$ and $93C^{\circ}$. Additionally, the temperature of the bottom calorimeter (and therefore the rod) was fixed at approximately 0 degrees C° while setting up the steady state. These temperatures were maintained on both calorimeters until a steady state temperature gradient was measured–when the temperature readings of both probes embedded in the rods were relatively constant. After the steady state condition was reached, the ice in the bottom calorimeter was removed, and all four temperatures were measured simultaneously for approximately 20 minutes. After the measurement was complete, the mass of the bottom calorimeter m_w was measured to be used as a constant in the formula for the thermal conductivity. This process was meticulously repeated for each of the three rods, and the change in temperature of the bottom rod thermal probe was plotted against time to determine the rate of change of total temperature in the rod $\frac{dT_{tot}}{dt}$.

With all relevant measurements needed to find the thermal conductivity λ taken, all measurements were substituted into formula 8 and the value of the thermal conductivity of Copper, Steel, and Aluminum were calculated.

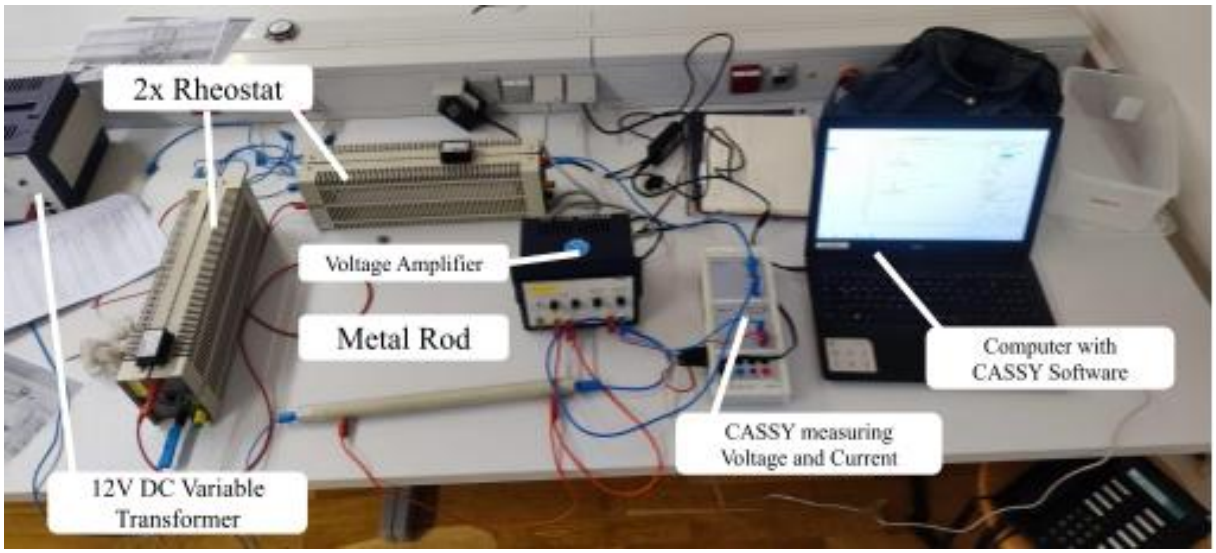

Figure 4: Setup to determine the Electrical Conductivity through the measurement of Resistance

To determine the electric conductivity of the three rods was a much simpler process than the determination of the thermal conductivity. A 12V DC variable transformer was passed into a Rheostat which behaved as a potential divider allowing for the variation of voltage across the rod. The second Rheostat was used as a variable resistor to increase and decrease the current running through the metal rod. By amplifying the measured voltage across the metal rod using a voltage amplifier (set to amplify by a factor of 10^4), and running the signal into the CASSY software, a linear plot was created between the voltage and the current measured in the metal rod, and the electric conductivity was determined. Figure 4 demonstrates the wiring of the setup necessary. Before taking any measurements, the voltage across the metal rod was set to 0 by moving the Rheostat as far downwards as possible. Then, the voltage amplifier was adjusted such that both the current and the voltage had values of zero. The leftmost rheostat (potential divider) was then moved all the way to the top, maximizing the voltage across the metal rod, and the variable resistor rheostat was configured such that the current through the metal rod was exactly 1.25 A. Then, after calibration, the variable resistor rheostat (top in figure) was fixed, and the potential divider (on left) was moved through 9 different Voltage Current configurations. As the resistance is trivially known (by Ohm's Law) to be the ratio of voltage over current $R = \frac{V}{I}$, the slope of the voltage (V) current (I) plot is the resistance (R), which was directly substituted into formula1 alongside the geometrical measurements for the rods–taken using a ruler and vernier calipers.

Lastly, the values of the electrical and thermal conductivites were divided over each other to assume the Wiedemann-Franz law (equation 2), and check the experimental adherence to the Lorenz number L value for the given room temperature the measurements were taken in (measured at the beginning and end of experiment to take arithmetic average).

4 Results and Data Analysis

To begin, the calefaction of water due to air was determined. Before the experiment, the absolute room temperature was measured to be $(296.45 \pm 0.1)K$. Furthermore, the mass of the empty calorimeter with the magnetic stirrer was determined to be $m_{empty}(0.24148 \pm 0.00001)kg$. The water was then cooled to $(0 \pm 0.1C^{\circ})$, which is equivalently defined as $273.15K$. Measurements of the temperature of the water in the calorimeter were taken every 30 seconds for 15 minutes. Below is the plot of the values measured for the temperature of the water in K.

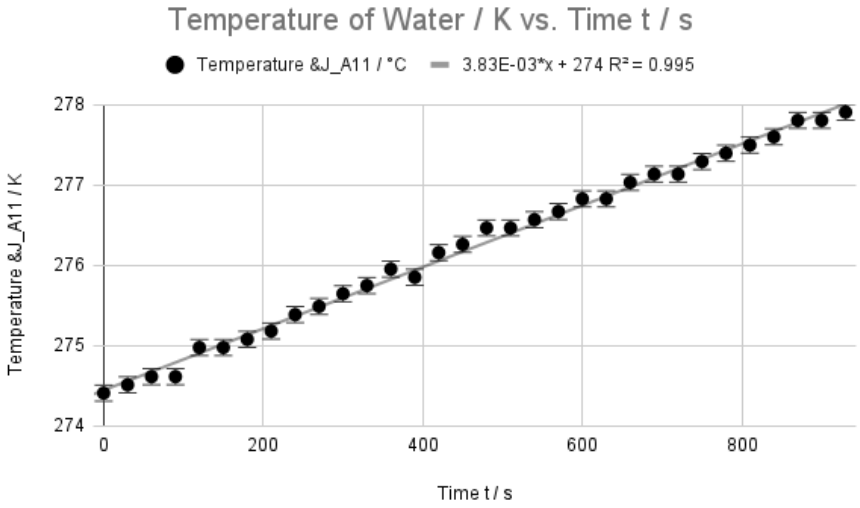

Figure 5: Plot of Temperature T of Water in the Calorimeter (K) against Time t (s)

After the measurement, the mass of the filled calorimeter was measured to be $((414.56 \pm 0.01) \cdot 10^{-3})kg$. The difference between the mass including the water and the calorimeter yields the total mass of the water used during the calefaction experiment:

$$m_{w,cf} = (173.08 \pm 0.02) \cdot 10^{-3} kg \tag{16}$$

The slope obtained from the graph $\frac{dT_{cf}}{dt}$ was calculated to be:

$$dT_{cf}/dt = (38.30 \pm 0.51) \cdot 10^{-4} [Ks^{-1}] \tag{17}$$

By substituting the newfound value of $\frac{dT_{cf}}{dt}$ into equation 11 and by applying the calculated specific heat capacity C of the calorimeter (from later experiment) dQ_R/dt value was calculated:

$$\frac{dQ_R}{dt} = (2.97 \pm 0.054)[J/s] \tag{18}$$

The next aspect of the experiment focused on performing a mixing experiment involving two different masses of hot and cold water. To calculate mass of the cold water in the stirring calorimeter, the mass of calorimeter filled with cold water was found, and the previously calcu-

lated mass of empty calorimeter m_{empty} was subtracted. To calculate mass of hot water used, the mass of the calorimeter filled with cold water was subtracted from the mass calorimeter filled with the mixture. The temperatures of all water masses were measured with respect to time such that the crucial values could be determined–the temperature of the separated hot and cold water just before mixing, and the average temperature of the mixture. With these values, they were substituted into equation 8 to directly obtain its' value, assuming the specific heat capacity of water c_w to be $\approx 4186[Jkg^{-1}K^{-1}]$. To find the error of the calculated specific heat capacity ΔC, partial derivative root sum of squares error propagation was used (RSS). This is discussed more extensively in the Error Analysis section of the report.

Experiment Number	**Experiment 1**	**Experiment 2**	**Experiment 3**	**Experiment 4**	**Experiment 5**
Mass of cold water ($\pm 1.0 \cdot 10^{-5}$) kg	0.20783	0.22943	0.19993	0.15960	0.20094
Mass of hot water ($\pm 2.0 \cdot 10^{-5}$) kg	0.18735	0.07965	0.20397	0.12713	0.13709
T_{cold} (± 0.1 K)	294.63	274.31	275.09	294.65	274.45
T_{hot} (± 0.1 K)	335.38	335.99	331.75	337.11	332.04
T_{mix} (± 0.1 K)	313.33	289.46	303.11	277.30	297.63
Calculated specific heat capacity ($J \cdot kg^{-1} \cdot K^{-1}$)	**54.58**	**63.71**	**35.66**	**11.08**	**10.79**
Error of calculated specific heat capacity	**10.61**	**10.54**	**7.29**	**7.85**	**7.48**

Table 1: Mixing Experiment Data and Calculated Specific Heat Capacity of Calorimeter C

From these 5 values of the specific heat capacity C obtained, the 3 that most closely adhered to the relevant theory were chosen. The three that were picked were the measurements taken during trials 1, 2 and 3—$54.58[Jkg^{-1}K^{-1}]$, $63.71[Jkg^{-1}K^{-1}]$, $35.66[Jkg^{-1}K^{-1}]$ respectively. Then, by taking the arithmetic mean of these 3 measurements, the final value of the specific heat capacity of the calorimeter was calculated to be:

$$C = \frac{54.58[Jkg^{-1}K^{-1}] + 63.71[Jkg^{-1}K^{-1}] + 35.66[Jkg^{-1}K^{-1}]}{3} \approx (51.3 \pm 9.4)[Jkg^{-1}K^{-1}] \tag{19}$$

The value of the calorimeters' specific heat capacity was then immediately applied to the first aspect of the investigation to derive the rate of calefaction due to the air $\frac{dQ_R}{dt}$ as aforementioned. The final result of the calefaction rate $\frac{dQ_R}{dt} = (2.97 \pm 0.054)[Js^{-1}]$ was found (see 18) using the calculated value for C. In preparation for the penultimate aspect of the investigation, the automatic control of the heating device was developed using a CASSY control parameter which conditionally activated for measured water temperatures below $90C°$. As the heat energy left in the metal caused the temperature to overshoot even after the heating was turned off, by prematurely disabling the heater at the condition of the temperature being lower than 90 degrees, the temperature of the water remained in a stable range between 90 and 93 degrees. The condition set on the CASSY was simple, just:

$$T_{A11} < 90 \tag{20}$$

The temperature T_{A11} in the condition above (20) refers to the temperature measured by the temperature probe submerged in the hot calorimeter. This condition allows one to maintain the consistently hot boundary condition temperatures necessary for generating the quasi-steady state for each rod during the measurement of the change in temperature of the metal rods as seen in figure 3.

Before measurement of the total change in temperature of the rod while in its quasi-steady state, geometric measurements of the rods were taken to be applied during the calculation of the thermal conductivity with formula 15. Additionally, the distance between the holes where the temperature probes were placed was noted to calculate the theoretical value of the temperature gradient $\frac{dT}{dx}$. Below denotes the table of geometric and mass values measured for each of the three rods, and the mass of the water in the bottom calorimeter (kg) after the measurements were taken.

Different rods:	**Copper**	**Aluminum**	**Steel**
Length of the rod ($\pm 10^{-3}$)m:	0.42	0.42	0.42
Distance between holes ($\pm 10^{-3}$)m:	0.315	0.315	0.315
Diameter ($\pm 5 \cdot 10^{-4}$)m:	0.026	0.026	0.0245
Radius($\pm 2.5 \cdot 10^{-4}$)m:	0.013	0.013	0.01225
Mass ($\pm 10^{-5}$)kg:	1.825	0.565	1.615
Volume ($\pm 6.65 \cdot 10^{-4}$)m^3:	0.034	0.034	0.032
Density ($\pm 5.65 \cdot 10^{-6}$)$kg \cdot m^{-3}$:	53.191	16.481	49.97
Mass of Water after Meas. ($\pm 10^{-5}$)kg:	0.604	0.7	0.683

Table 2: Measured Geometric Properties of Copper Aluminum and Steel Rods

Using these values, the cross sectional of each rod was calculated as:

$$A_{Copper} = (5.31 \pm 0.64) \cdot 10^{-4}[m^2] \tag{21}$$

$$A_{Aluminum} = (5.31 \pm 0.64) \cdot 10^{-4}[m^2] \tag{22}$$

$$A_{Steel} = (4.71 \pm 0.59) \cdot 10^{-4}[m^2] \tag{23}$$

The rods were first brought to their steady state conditions by waiting until the temperatures measured by the two temperature probes embedded in the rods were stable. after this stability was reached, it was clear a steady state condition (with a linear temperature gradient) was generated. To then measure the change in temperature of the bottom rod-embedded temperature probe, the ice in the bottom calorimeter was removed to allow for the bottom temperature of the rod to change. This change in temperature C° was measured and plotted against time s, and a linear positive growth trend was examined. Below are the plots of the temperature in Celsius against time for Steel, Copper and Aluminum respectively.

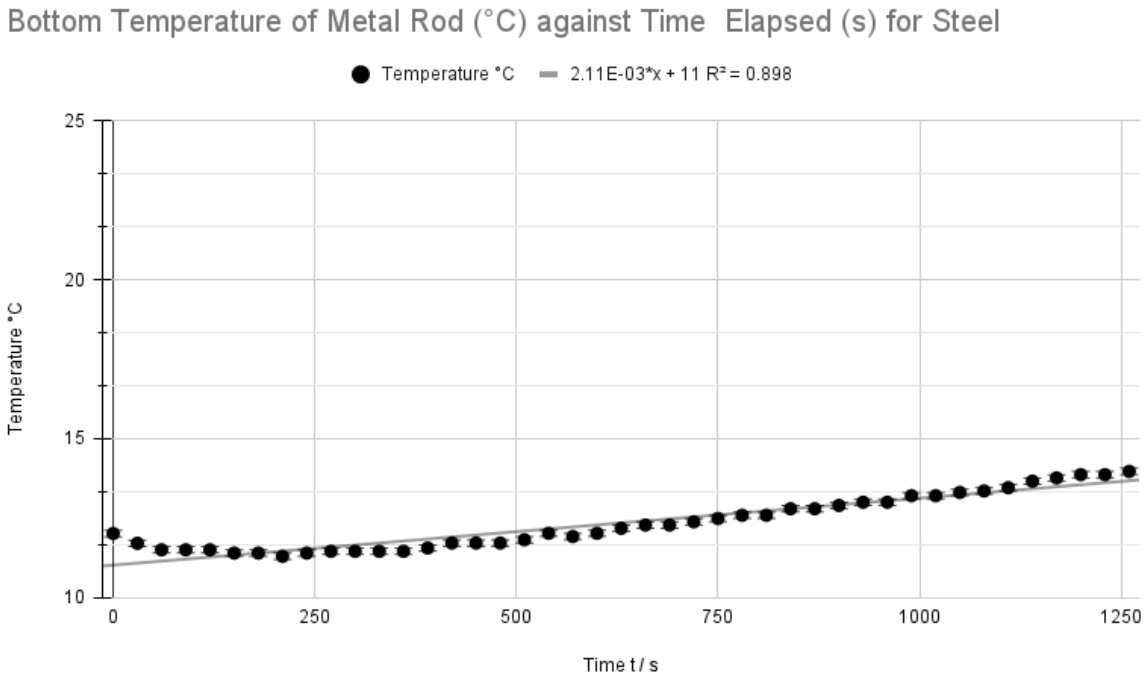

Figure 6: Total Temperature Variation Graph for Steel

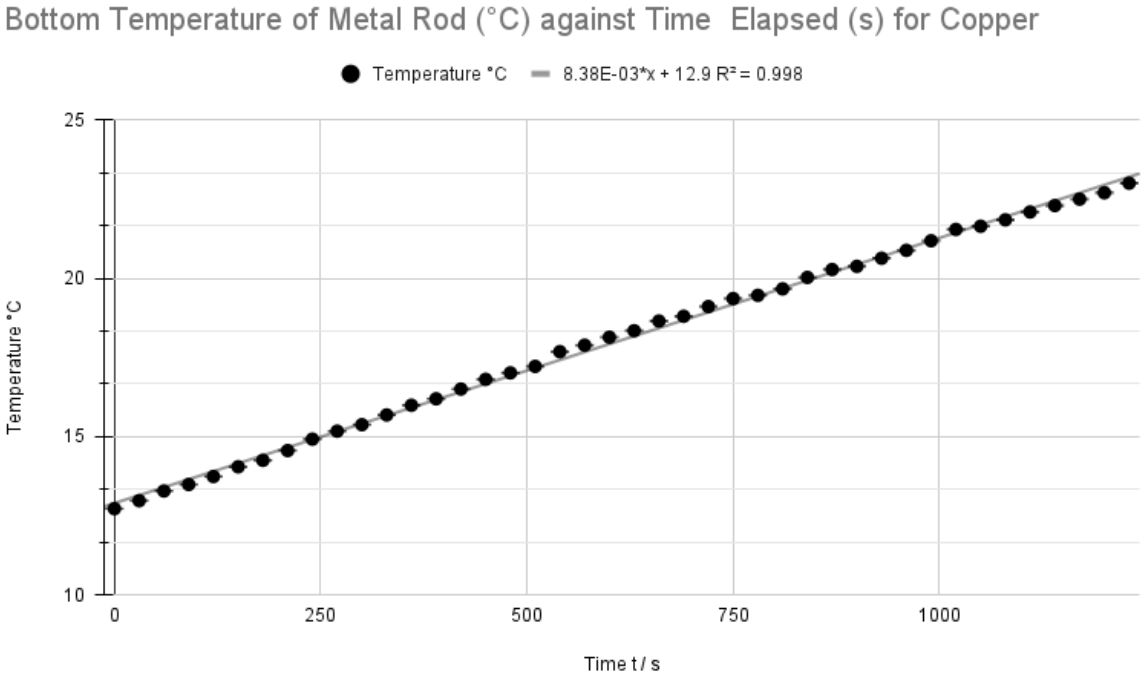

Figure 7: Total Temperature Variation Graph for Copper

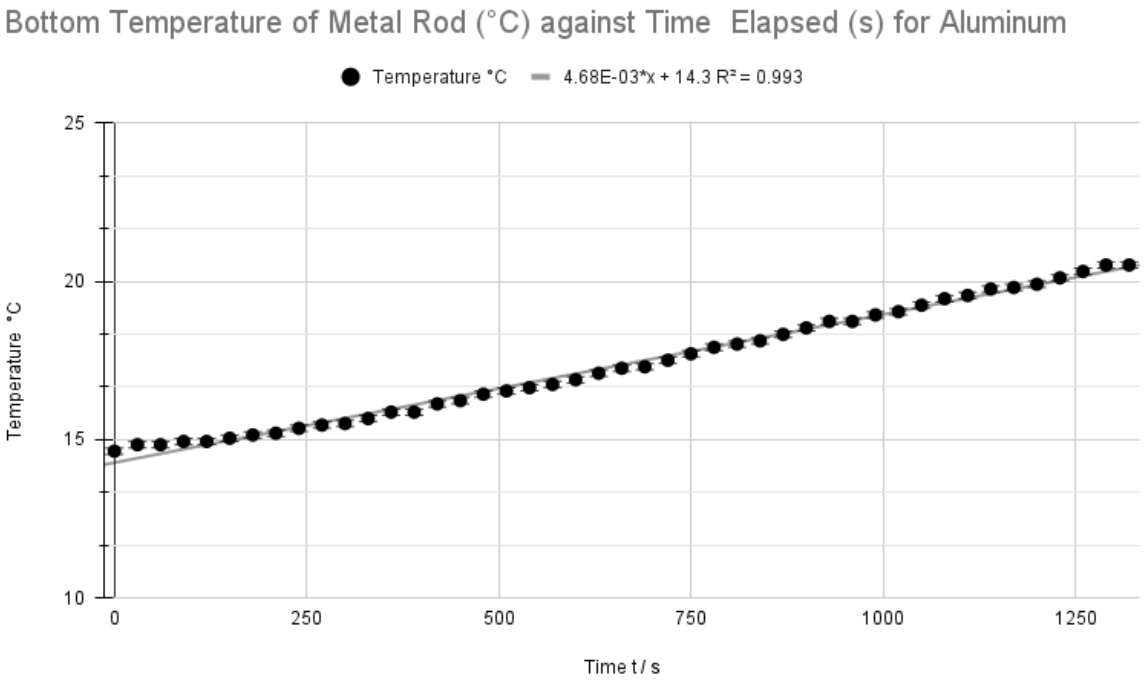

Figure 8: Total Temperature Variation Graph for Aluminum

As one can observe from figures 6, 7 and 8, a strong linear correlation is present in the data of all three rods and the slope varies depending on the metal used. This is expected, as depending on the thermal conductivity λ of the rod, the rate of heat energy change $\frac{dQ}{dt}$–which is correlated directly to temperature change through equation 13–is linearly dependent on the thermal conductivity of the metal (seen in equation 5). From these graphs the rates of change of total temperature $\frac{dT_{tot}}{dt}$ are extracted for Steel, Copper and Aluminum respectively. The values of the change in total temperature $\frac{dT_{tot}}{dt}$ are given as:

$$\frac{dT_{tot}}{dt}_{Steel} = (8.838 \pm 0.059) \cdot 10^{-3}[C°/s] \tag{24}$$

$$\frac{dT_{tot}}{dt}_{Copper} = (4.68 \pm 0.058) \cdot 10^{-3}[C°/s] \tag{25}$$

$$\frac{dT_{tot}}{dt}_{Aluminum} = (2.11 \pm 0.11) \cdot 10^{-3}[C°/s] \tag{26}$$

With the final calculated values for the change in temperature with respect to time, one can trivially calculate the thermal conductivity constants of Copper, Aluminum and Steel through the substitution of known values into equation 15. Below is a sample calculation which uses the known values of the specific heat capacity of the calorimeter, rate of calefaction, initial temperatures (taken from graph) and the geometric measurements to find the thermal conductivity λ of the copper rod.

$$\lambda_{copper} = \frac{(c_w \cdot m_w + C)\frac{dT_{tot}}{dt}|_{T_0} - (c_w \cdot m_{w,cf} + C) \cdot \frac{dT_{cf}}{dt}|_{T_0}}{-A \cdot \frac{T_2 - T_1}{l}}$$

Substituting all values obtained throughout the investigation, a long expression is obtained.

$$\lambda_{\text{Copper}} = \frac{\left((4186[Jkg^{-1}K^{-1}] \cdot 0.604[kg] + 51.3[Jkg^{-1}K^{-1}]\right) \cdot 4.68 \cdot 10^{-3}[C^{\circ}s^{-1}] - \left(4186[Jkg^{-1}K^{-1}] \cdot 173.08 \cdot 10^{-3}[kg] + 51.3[Jkg^{-1}K^{-1}]\right) \cdot 38.3 \cdot 10^{-4}[Ks^{-1}]}{-5.31 \cdot 10^{-4}\,[m^2] \cdot \frac{12.7[C^{\circ}] - 45.2[C^{\circ}]}{0.315[m]}} \tag{27}$$

When numerically computed, the final value becomes:

$$\implies \lambda_{Copper} = (340.9 \pm 13.6)[Wm^{-1}K^{-1}] \tag{28}$$

Again, the error for this measurement was calculated using partial differentiation root sum of squares (RSS). This process is further elaborated upon in the Error Analysis section of the report. In a similar fashion to the computation of the thermal conductivity of the copper, rod, the same calculations were performed to find the thermal conductivities of steel and aluminum as well. The three final calculated values for the thermal conductivities $\lambda_{Steel}, \lambda_{Copper}$ and $\lambda_{Aluminum}$ are:

$$\lambda_{Steel} = (46.4 \pm 5.16)[Wm^{-1}K^{-1}] \tag{29}$$

$$\lambda_{Copper} = (340.9 \pm 13.6)[Wm^{-1}K^{-1}] \tag{30}$$

$$\lambda_{Aluminum} = (161.5 \pm 6.8)[Wm^{-1}K^{-1}] \tag{31}$$

Examining the thermal conductivities of the three metals, it is clear that Copper has the largest thermal conductivity. As a hypothesis, and by the pseudo-constant nature of the ratio of thermal and electrical conductivities, it can be reasonably assumed that the electrical conductivity of copper will also be the highest, and the electrical conductivity of steel will be the lowest.

To determine the electrical conductivity of the metal rods, the relationship between the voltage (V) and current (I) was examined across all three rods in order to determine the resistance (R). By pairing the resistance measurement with the geometrical measurements of the rods calculated during the measure of thermal conductivity, the electrical conductivity was determined from equation 1. First, the voltage was zeroed out at the lowest potential division. The amplifier was set to an amplification order of $10^{-4}V$. Then, the voltage was maximized via the configuration of the rheostat at its maximum. The variable resistor rheostat was configured in such a way that the current through the metal rod was at a maximum of $1.25[A]$. The voltage was then measured alongside the current through 9 distinct values between the maximum voltage and 0. The data collected by the CASSY system was then plotted on a graph with the Amplified Voltage (V) against Current (I). Below are the three plots which demonstrate this relationship for Steel, Copper and Aluminum rods respectively.

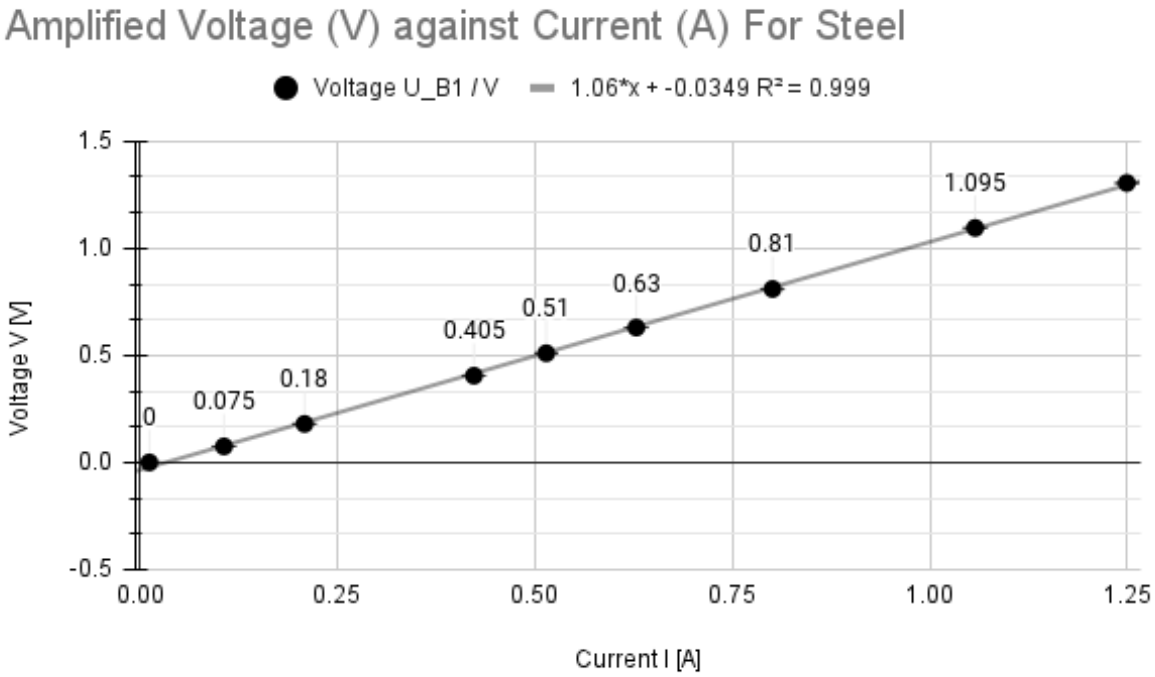

Figure 9: Plot of the Amplified Voltage (V) against the current through Steel Rod

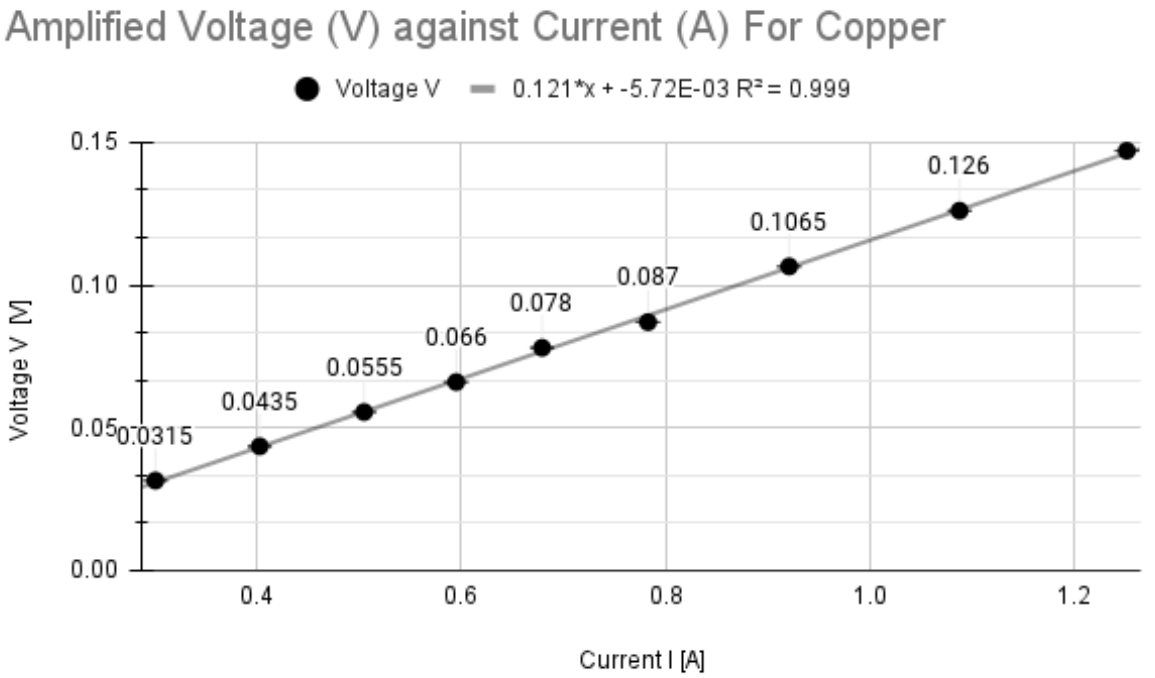

Figure 10: Plot of the Amplified Voltage (V) against the current through Copper Rod

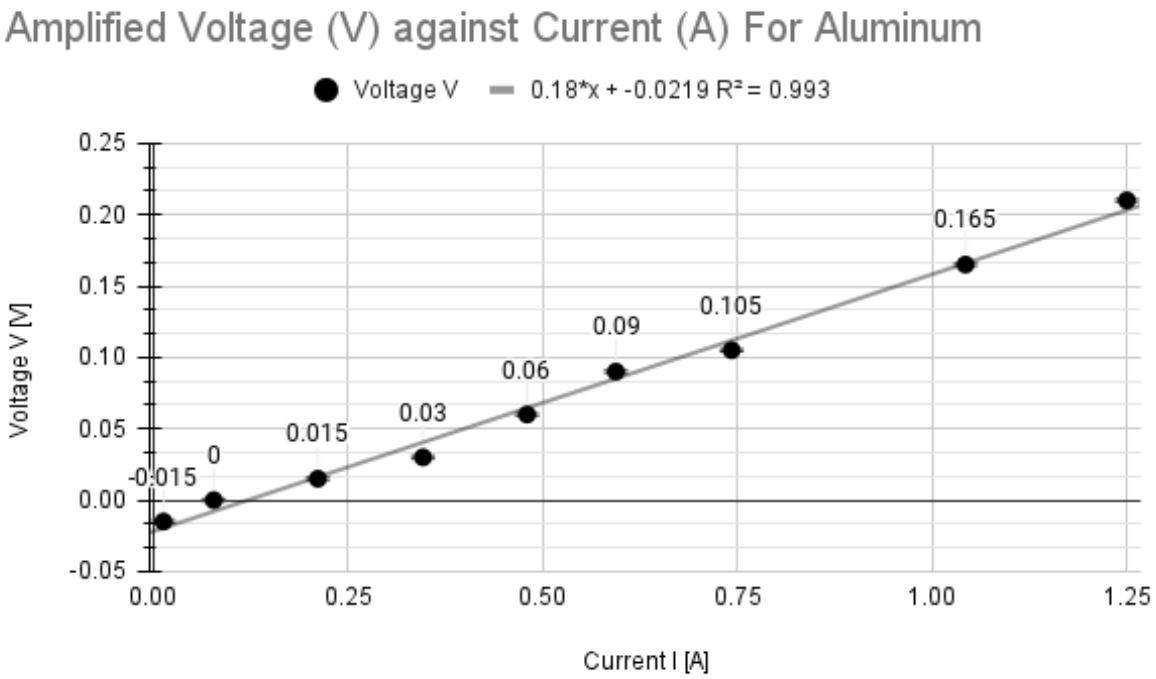

Figure 11: Plot of the Amplified Voltage (V) against the current through Aluminum Rod

The above plots demonstrate a strong linear correlation between the Voltage and the Current propagating through the metal rods. By analyzing the gradient of the graph, the Resistance can be determined directly. Below are the 3 extracted values for the total resistance R along the metal rods for Steel, Copper and Aluminum respectively, accounting for the amplification of the voltage (10^4).

$$R_{steel} = (1.06 \pm 0.00924) \cdot \underbrace{10^{-4}}_{\text{Amp.}}[\Omega] \tag{32}$$

$$R_{copper} = (0.121 \pm 0.00125) \cdot \underbrace{10^{-4}}_{\text{Amp.}}[\Omega] \tag{33}$$

$$R_{aluminum} = (0.18 \pm 0.00575) \cdot \underbrace{10^{-4}}_{\text{Amp.}}[\Omega] \tag{34}$$

Substituting these values into equation 1, one achieves the following electrical conductivities σ for Steel, Copper and Aluminum respectively, taking geometrical values from table 2. Below are the calculated values for the electrical conductivities σ.

$$\sigma_{steel} = \frac{l}{A \cdot R} = \frac{0.42[m]}{4.71 \cdot 10^{-4}[m^2] \cdot 1.06 \cdot 10^{-4}[\Omega]} = (8.40 \pm 0.69) \cdot 10^6[Sm^{-1}] \tag{35}$$

$$\sigma_{copper} = \frac{l}{A \cdot R} = \frac{0.42[m]}{5.31 \cdot 10^{-4}[m^2] \cdot 1.21 \cdot 10^{-5}[\Omega]} = (6.54 \pm 0.51) \cdot 10^7[Sm^{-1}] \quad (36)$$

$$\sigma_{aluminum} = \frac{l}{A \cdot R} = \frac{0.42[m]}{5.31 \cdot 10^{-4}[m^2] \cdot 0.18 \cdot 10^{-4}[\Omega]} = (4.29 \pm 0.338) \cdot 10^7[Sm^{-1}] \quad (37)$$

From the results above, it is clear that copper has the highest electrical conductivity, matching theoretical prediction. A high electrical conductivity means that it is often the clear choice for use in electrical applications, as it provides the least resistance, also demonstrated by the results. Steel on the other hand, has a relatively lower electrical conductivity, likely due to it's higher resistance and smaller mean free path for the electrons in its crystal lattice (as they are closer together as a denser metal).

With both the thermal and electrical conductivities calculated, one can attempt to calculate the Lorenz number L using the constant calculated during the experiment, λ and σ. The Wiedemann-Franz law connects the thermal and electrical conductivities of a metal to the Lorenz number, which is defined as $L = \frac{\pi^2}{3} \cdot \frac{k_B^2}{e^2}$, where k_B is Boltzmann's constant, and e is the elementary charge. Solving the Wiedemann-Franz law for the Lorenz number in terms of the conductivities and the room temperature the experiment was performed in, one achieves an expression of the Lorenz number L as follows from equation 2:

$$L = \frac{\lambda}{\sigma \cdot T_0} \quad (38)$$

The corresponding experimentally determined values of the Lorenz number for Steel, Copper and Aluminum are listed below, respectively:

$$L_{Steel} = \frac{46.4[Wm^{-1}K^{-1}]}{8.4 \cdot 10^6[Sm^{-1}] \cdot 296.75[K]} = (1.86 \pm 0.368) \cdot 10^{-8}[W\Omega K^{-2}] \quad (39)$$

$$L_{Copper} = \frac{340[Wm^{-1}K^{-1}]}{6.54 \cdot 10^7[Sm^{-1}] \cdot 296.75[K]} = (1.76 \pm 0.22) \cdot 10^{-8}[W\Omega K^{-2}] \quad (40)$$

$$L_{Aluminum} = \frac{161.5[Wm^{-1}K^{-1}]}{4.39 \cdot 10^7[Sm^{-1}] \cdot 296.75[K]} = (1.24 \pm 0.15) \cdot 10^{-8}[W\Omega K^{-2}] \quad (41)$$

Given that the Lorenz number $L \approx 2.4 \cdot 10^{-8}[W\Omega K^{-2}]$, the values obtained are close to, but not fully adherent to the literature/theoretical value. This is likely due to a multitude of causes and errors present throughout the experimental method, which will be discussed now.

5 Error Analysis

For all errors involving the slope of the graph, the uncertainty of the slope was approximated using the built-in function (LINEST), which works by approximating the linear slope of a set of data points through the least squares method. As a byproduct, the error of the slope is given in absolute form. Due to the efficiency of this method, and the large quantity of graphs, it was the clear choice for this investigation. For all errors involving numerical calculations with propagated error, such as for the uncertainties of the final measurements, the root sum of squares method (RSS) was employed. This method involves calculating the propagated error of a formulaic value by computing all partial derivatives with respect to all error prone parameters, and taking it under a square root. The formula for this is given below.

$$\Delta y = \sqrt{\sum_{i=0}^{n} \left(\frac{\partial y}{\partial x_i} \cdot \Delta x_i \right)^2} = \sqrt{\left(\frac{\partial y}{\partial x_1} \cdot \Delta x_1 \right)^2 + \cdots + \left(\frac{\partial y}{\partial x_n} \cdot \Delta x_n \right)^2} \tag{42}$$

The instrumental error of all temperature measurements taken by the CASSY system was $\pm 0.1 C^{\circ}$. For mass measurements, the instrumental error was taken as $\pm 10^{-5} kg$ (instrumental error of the mass scale). Regarding the calculated mass of the cold water, the error of the mass scale was doubled as the subtraction of two measurements was taken–the mass of the calorimeter without and with water. The error determined for the mass of the hot water was $2 * 10^{-5} kg$. The error of the rate of calefaction $\frac{dQ}{dt}$ and error of the specific heat capacity C of the calorimeter was calculated using RSS method, as previously introduced. Below is the calculated RSS error propagation for the rate of calefaction $\frac{dQ}{dt}$:

$$\Delta(dQ/dt) = \sqrt{\left(c_w \cdot \frac{dT_{cf}}{dt} \cdot \Delta m_{w,cf} \right)^2 + \left(\frac{dT_{cf}}{dt} \cdot \Delta C \right)^2 + \left((c_w \cdot m_{w,cf} + C) \cdot \Delta \frac{dT_{cf}}{dt} \right)^2} \tag{43}$$

Note however that this equation uses the error of the specific heat capacity of the calorimeter ΔC. This value also needs to be propagated in a similar fashion by taking the partial derivatives of equation 8 with respect to all error prone values. Below is the equation of the propagated error for the specific heat capacity of the calorimeter.

$$\Delta C = \sqrt{\left(\frac{\partial C}{\partial m_{w,\text{hot}}} \Delta m_{w,\text{hot}} \right)^2 + \left(\frac{\partial C}{\partial m_{w,\text{cold}}} \Delta m_{w,\text{cold}} \right)^2 + \left(\frac{\partial C}{\partial T_{\text{hot}}} \Delta T_{\text{hot}} \right)^2 + \left(\frac{\partial C}{\partial T_{\text{mix}}} \Delta T_{\text{mix}} \right)^2 + \left(\frac{\partial C}{\partial T_{\text{cold}}} \Delta T_{\text{cold}} \right)^2 + \left(\frac{\partial C}{\partial T_{\text{cal}}} \Delta T_{\text{cal}} \right)^2} \tag{44}$$

The partial derivative terms inside of the function are for the masses of the hot and cold water, temperature of the hot and cold and mixed water, and the temperature of the calorimeter. Below denotes the calculated partial derivatives of equation 8, multiplied by the instrumental error associated with each partial derivative:

$$\frac{\partial C}{\partial m_{w,\text{hot}}}\Delta m_{w,\text{hot}} = \frac{c_w(T_{\text{hot}} - T_{\text{mix}})}{T_{\text{mix}} - T_{\text{cal}}} \cdot \Delta m_{w,\text{hot}} \tag{45}$$

$$\frac{\partial C}{\partial m_{w,\text{cold}}}\Delta m_{w,\text{cold}} = \frac{-c_w(T_{\text{mix}} - T_{\text{cold}})}{T_{\text{mix}} - T_{\text{cal}}} \cdot \Delta m_{w,\text{cold}} \tag{46}$$

$$\frac{\partial C}{\partial T_{\text{hot}}}\Delta T_{\text{hot}} = \frac{c_w m_{w,\text{hot}}}{T_{\text{mix}} - T_{\text{cal}}} \cdot \Delta T_{\text{hot}} \tag{47}$$

$$\frac{\partial C}{\partial T_{\text{mix}}}\Delta T_{\text{mix}} = \left(\frac{c_w m_{w,\text{cold}} + c_w m_{w,\text{hot}}}{T_{\text{mix}} - T_{\text{cal}}} - \frac{c_w m_{w,\text{hot}}(T_{\text{hot}} - T_{\text{mix}}) - c_w m_{w,\text{cold}}(T_{\text{mix}} - T_{\text{cold}})}{(T_{\text{mix}} - T_{\text{cal}})^2}\right) \cdot \Delta T_{\text{mix}} \tag{48}$$

$$\frac{\partial C}{\partial T_{\text{cold}}}\Delta T_{\text{cold}} = \frac{c_w m_{w,\text{cold}}}{T_{\text{mix}} - T_{\text{cal}}} \cdot \Delta T_{\text{cold}} \tag{49}$$

$$\frac{\partial C}{\partial T_{\text{cal}}}\Delta T_{\text{cal}} = (-\frac{c_w m_{w,\text{hot}}(T_{\text{hot}} - T_{\text{mix}}) - c_w m_{w,\text{cold}}(T_{\text{mix}} - T_{\text{cold}})}{(T_{\text{mix}} - T_{\text{cal}})^2}) \cdot \Delta T_{\text{cal}} \tag{50}$$

When determining the physical properties of the Copper, Aluminum and Steel, the ruler had an instrumental error of $0.5 \cdot 10^{-3} m$. The errors of the density and volume of the rod were calculated using RSS method again as:

$$\Delta V = 2\pi\sqrt{(l\Delta r)^2 + (r\Delta l)^2} \tag{51}$$

$$\Delta\rho = \sqrt{\left(\frac{\Delta m}{V}\right)^2 + \left(\frac{m\Delta V}{V^2}\right)^2} \tag{52}$$

After the errors of the volume and density of the rods were calculated, the errors of the thermal and electrical conductivities were obtained through the same method, as seen below:

$$\Delta\lambda = \sqrt{\left(\frac{\partial\lambda}{\partial m_w}\Delta m\right)^2 + \left(\frac{\partial\lambda}{\partial m_{w,cf}}\Delta m_{w,cf}\right)^2 + \left(\frac{\partial\lambda}{\partial(k_1)}\Delta k_1\right)^2 + \left(\frac{\partial\lambda}{\partial(k_2)}\Delta k_2\right)^2 + \left(\frac{\partial\lambda}{\partial(T_2 - T_1)}\Delta(T_2 - T_1)\right)^2 + \left(\frac{\partial\lambda}{\partial r}\Delta r\right)^2 + \left(\frac{\partial\lambda}{\partial l}\Delta l\right)^2 + \left(\frac{\partial\lambda}{\partial C}\Delta C\right)^2} \tag{53}$$

Where $k_1 = dT_{tot}/dt$ and $k_2 = dT_{cf}/dt$, $T_2 - T_1$ is treated as one variable to simplify the expression.

$$\Delta\sigma = \sqrt{\left(\frac{1}{\pi r^2 R}\Delta l\right)^2 + \left(-\frac{2l}{\pi r^3 R}\Delta r\right)^2 + \left(-\frac{l}{\pi r^2 R^2}\Delta R\right)^2} \tag{54}$$

Where ΔR value was obtained from the LINEST function of the Amplified Voltage agains Current graph. ”l” and ”r” are measured with ruler so they contain instrumental error of the ruler. To estimate the uncertainty in L the propagation of uncertainties method was used. This involves calculating the partial derivatives of L with respect to each variable k, σ and T_0 and then combining these with their respective uncertainties, which were already calculated:

$$\Delta L = L(\frac{\Delta\lambda}{\lambda} + \frac{\Delta\sigma}{\sigma} + \frac{\Delta T_0}{T_0}) \tag{55}$$

6 Discussion

The results for the thermal conductivity λ and electrical conductivity σ calculated during the investigation are:

Experimental Thermal Conductivities

$$\lambda_{steel} = (46.4 \pm 5.16)[Wm^{-1}K^{-1}] \tag{56}$$

$$\lambda_{copper} = (340.9 \pm 13.6)[Wm^{-1}K^{-1}] \tag{57}$$

$$\lambda_{aluminum} = (161.5 \pm 6.8)[Wm^{-1}K^{-1}] \tag{58}$$

Experimental Electrical Conductivities

$$\sigma_{steel} = (8.40 \pm 0.69) \cdot 10^{6}[Sm^{-1}] \tag{59}$$

$$\sigma_{copper} = (6.54 \pm 0.51) \cdot 10^{7}[Sm^{-1}] \tag{60}$$

$$\sigma_{aluminum} = (4.29 \pm 0.338) \cdot 10^{7}[Sm^{-1}] \tag{61}$$

Furthermore, the literary values of the thermal conductivity λ and the electrical conductivity σ of steel, copper and aluminum are given by:

Theoretical Thermal Conductivities (Young, 1992)

$$\lambda_{steel,theory} = (50.2)[Wm^{-1}K^{-1}] \tag{62}$$

$$\lambda_{copper,theory} = (385)[Wm^{-1}K^{-1}] \tag{63}$$

$$\lambda_{aluminum,theory} = (205)[Wm^{-1}K^{-1}] \tag{64}$$

Theoretical Electrical Conductivities (Anne Marie Helmenstine, 2002)

$$\sigma_{steel,theory} = 1.45 \cdot 10^{6}[Sm^{-1}] \tag{65}$$

$$\sigma_{copper,theory} = 5.96 \cdot 10^{7}[Sm^{-1}] \tag{66}$$

$$\sigma_{aluminum,theory} = 3.5 \cdot 10^{7}[Sm^{-1}] \tag{67}$$

Comparing the theoretical values above, it is clear that are results are marginally inconsistent with the predicted theoretical values. While the overall trend is the same, copper having the largest predicted conductivity in both thermal and electrical cases, the data falls outside of the theoretical margin for some of the measurements taken. The measurement series where this error is most notable are the electric conductivities of the metals. One can explain the deviation in measured value from the theoretical value for many reasons. The most probable cause, which was due to lack of realization, was the temperature of the rod. As the electrical conductivity setup immediately followed the measurement of the thermal conductivity, the temperature of

the rods may have been skewed from their expected value of room temperature. This would introduce major systematic error causing the values of the electrical conductivity to appear greater than what was theoretically predicted (by the Wiedemann-Franz law, equation 2). In the future, an intermediate step should be implemented into the method which regulates the temperatures of the rods before being used in a measurement of electrical conductivity. This systematic shift is clearly evident in the data, as every electrical conductivity calculated is by a significant margin larger than the predicted value.

For the thermal conductivity, the error introduced was also somewhat systematic, as every value measured appears to be smaller than the predicted value (see above). After careful examination of the method, the most probable cause of this systematic error is due to the causal systematic error in the calculation of the specific heat capacity of the calorimeter. During the mixing experiment, the temperature of the hot water was measured by placing a temperature probe into the water alongside the heating module. As seen in the figure of setup 2 (figure 2), the heated calorimeter was not equipped with a stirring stick, potentially leading to an uneven temperature distribution in the calorimeter. Additionally, due to the size of the calorimeter, it was difficult to sufficiently isolate the heating element and the thermal probe from one another, and it is likely that the temperature probe measured consistently higher values for the water due to its close proximity (touching) to the heating element. This systematic error is exactly what one observes from the above values.

The theoretical value of the Lorenz number is $L \approx 2.4 \cdot 10^{-8}[W\Omega K^{-2}]$. The values obtained for steel, copper, and aluminum respectively were:

$$L_{steel} = (1.86 \pm 0.368) \cdot 10^{-8}[W\Omega K^{-2}] \tag{68}$$

$$L_{copper} = (1.76 \pm 0.22) \cdot 10^{-8}[W\Omega K^{-2}] \tag{69}$$

$$L_{aluminum} = (1.24 \pm 0.15) \cdot 10^{-8}[W\Omega K^{-2}] \tag{70}$$

Immediately, it is clear that the Lorenz numbers calculated are less than the theoretical value by quite a significant margin. Analyzing the way in which the systematic error in both the thermal and electrical conductivity would propagate to the calculated value of the Lorenz number, the systematic error makes sense. The formula for the Lorenz number derived from the Wiedemann-Franz law is given by:

$$L = \frac{\lambda}{\sigma \cdot T_0} \tag{71}$$

As the measured thermal conductivity λ is less than the theoretical value, and the measured electrical conductivity σ is greater than the theoretical value, it is clear by the two parameters' location in the equation that it would lead to an even farther undershot value of the Lorenz number L. The deviations in the thermal and electrical conductivities are the clear cause of the apparent systematic error in the calculated Lorenz number.

To suggest an alternative method which takes into account the thermal dependent of the electrical conductivity, it would be important to introduce an intermediate step in the method between the calculation of the thermal and electrical conductivities. A 'cooldown' phase for the rods would be beneficial in ensuring that the temperature measured at for the electrical conductivity is room temperature. This is very important, as highlighted by the linear dependence on temperature in the Wiedemann-Franz law. In addition, a larger calorimeter should be used to allow the separation of the heater and the temperature probe more. As an alternative, the heating element could be removed, and then the water could be stirred manually using the temperature prove. The stirring would provide an even distribution and there would be no systematic offsets due to the heater. Overall, the measurements obtained during the investigation accurately portray the relative difference between the 3 metals in question, however only weakly adhere to the theoretical values due to the presence of 2 main unconsidered systematic sources of error.

7 Conclusion

In this investigation, the heat capacity of a calorimeter and the thermal and electrical conductivities of Copper, Aluminium and Steel were calculated alongside the Lorenz Number. The experiment combined measurements of the temperature of the rods in static thermal equilibrium, and the measurement of the resistance of the rods. The error analysis of the results ensured the reliability of the results. Conducting a mixing experiment which combined hot and cold water into a calorimeter, the specific heat capacity of the calorimeter was found through the conservation of energy to be $C = 51.316 \pm 9.478[Jkg^{-1}K^{-1}]$.

The thermal conductivity values of the copper, aluminum and steel were determined to be: $(340.9 \pm 13.16)Wm^{-1}K^{-1}$, $(161.5 \pm 6.8)Wm^{-1}K^{-1}$ and $(46.4 \pm 5.15)Wm^{-1}K^{-1}$ respectively. These values are consistent with high thermal conductivity expected for Copper and Aluminum and the lower value for Steel. The discrepancies can be caused because of prominent systematic errors, and minor environmental factors. The electrical conductivity of the materials was determined as: $\sigma_{steel} = (8.40 \pm 0.69) \cdot 10^6[Sm^{-1}]$,$\sigma_{copper} = (6.54 \pm 0.51) \cdot 10^7[Sm^{-1}]$,$\sigma_{aluminum} = (4.29 \pm 0.338) \cdot 10^7[Sm^{-1}]$.

These measurements align well with the known electrical properties of the materials, highlighting the superiority of the conductivity of Copper, followed by Aluminum and Steel. Then the Lorenz Number was calculated based on each material: $L_{steel} = (1.86 \pm 0.368) \cdot 10^{-8}[W\Omega K^{-2}]$,$L_{copper} = (1.76 \pm 0.22) \cdot 10^{-8}[W\Omega K^{-2}]$,$L_{aluminum} = (1.24 \pm 0.15) \cdot 10^{-8}[W\Omega K^{-2}]$.

The Lorenz Numbers found are slightly lower than the theoretical value of $2.410^{-8}[W\Omega K^{-2}]$, but the values still reflect the systematic errors in the thermal and electrical conductivity. The deviation from the theoretical value suggests that corrections to the method should be made, such as ensuring equalized temperatures of the rods during the electric experiment and the investigation of the effects of varying environmental conditions.

Overall, the obtained values in general are in reasonable agreement with theoretical expectations and literature values. They contribute to a better understanding of thermal and electrical properties of different materials and investigating the factors affecting conductivity.

References

Anne Marie Helmenstine, P. (2002, May). *Table of electrical resistivity and conductivity.* ThoughtCo. Retrieved from https://www.thoughtco.com/table-of-electrical-resistivity-conductivity-608499

Wagner, V., & Söcker, T. J. (2024). Advanced physics lab 1 manual. *Constructor University*.

Young, H. D. (1992). *University physics* (7th ed.). Addison Wesley.